Electronic Supplementary Material (ESI) for Dalton Transactions

Supporting information

for

An Iron(III) Tetradentate Monoamido Complex as a Nonheme Iron-Based Peroxidase Mimetic

Yutaka Hitomi*, Kazuaki Hiramatsu, Kengo Arakawa,
Toshiyuki Takeyasu, Masashi Hata, and Masahito Kodera
Department of Molecular Chemistry and Biochemistry, Doshisha University
1-3 Tatara Miyakodani, Kyototanabe, Kyoto 610-0321, Japan
yhitomi@mail.doshisha.ac.jp

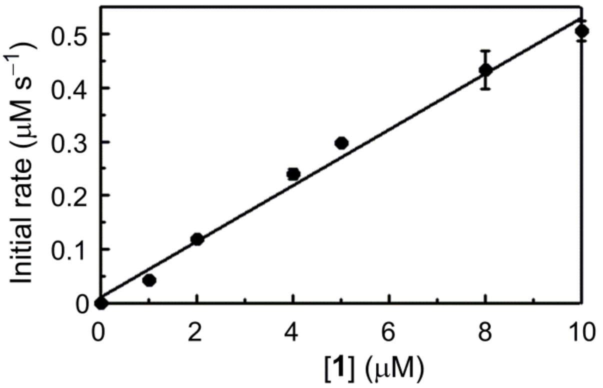

Fig S1. Dependence of the initial rates of the oxidation of ABTS (20 μM) with 1 mM H_2O_2 on the concentration of **1**.

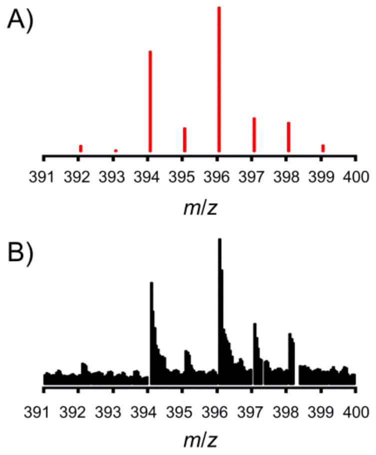

Fig S2. CSI-MS spectra of a reaction mixture of **1** and 100 equiv. of H_2O_2 (B) in $CH_3CN/^{18}O$-labeled H_2O (9:1) at 0°C. The isotope pattern shown in panel A is assignable to a mixture of unlabeled species at *m*/*z* 394.2, mono-^{18}O-labeled species at *m*/*z* 396.2, and $[Fe^{III}(mpaq)Cl]^+$ at *m*/*z* 396 and 398 (39.3:27.3:33.3), whose simulated spectrum is shown in panel A.

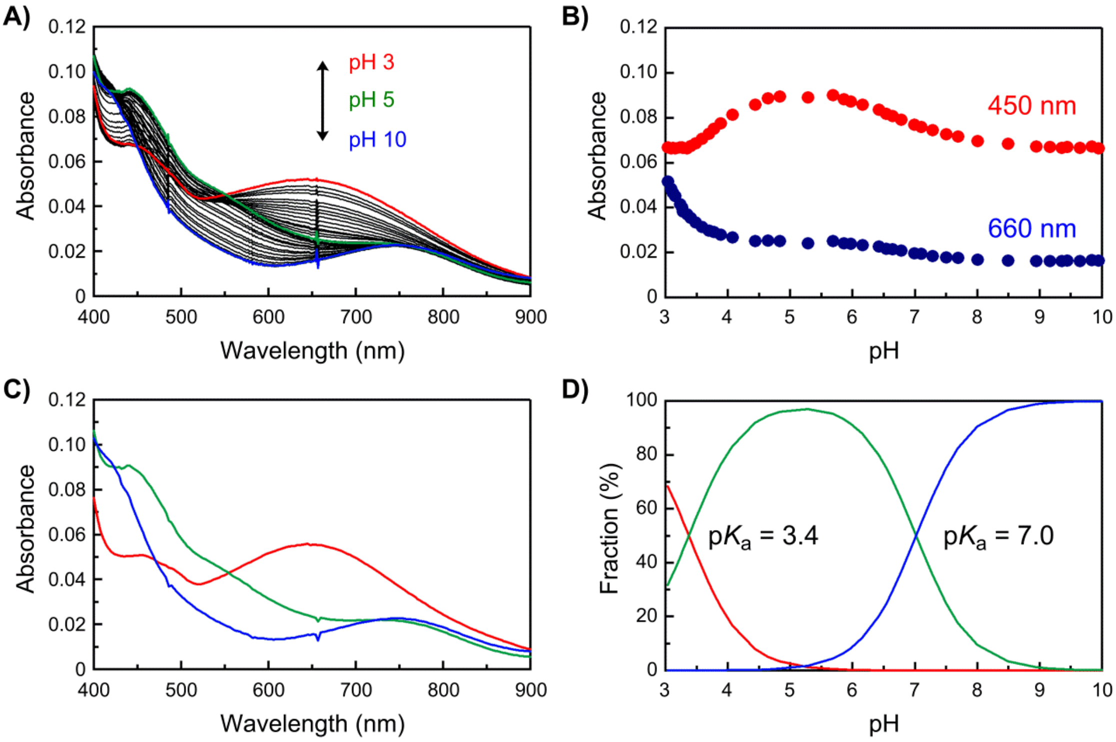

Fig S3. UV–vis spectral change of **1** in H_2O at varied pH values. [**1**] = 0.125 mM. Panel B shows the absorbance at 450 and 660 nm against pH value. Panel C shows the spectra of three species determined by singular value decomposition analysis using the program SPECFIT. Panel D shows the mole fractions of the three species against pH values.

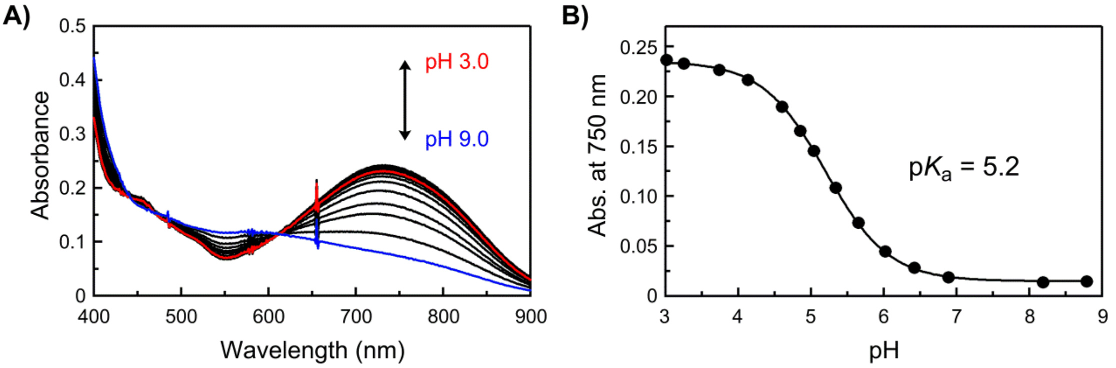

Fig S4. UV–vis spectral change of **2** in H_2O at varied pH values. Panel B shows the absorbance at 750 nm against pH value. [**2**] = 0.25 mM. The solid line is a fitted curve by using the following equation; $A_{obs} = (A_{max} \times 10^{pH\text{-}pKa} + A_{min})/(1 + 10^{pH\text{-}pKa})$.

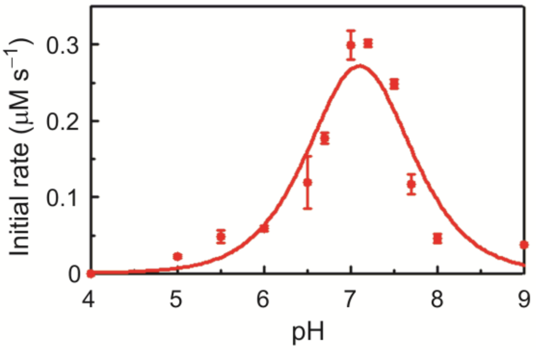

Fig S5. pH dependence of the initial reaction rate for the decomposition of Orange II (20 μM) using H_2O_2 (0.5 mM) in the presence of 2.0 μM **1**. The solid line is a fitted curve by using the following equation; $v = v_{max}/(1 + 10^{pKa1-\,pH} + 10^{pH-pKa2})$ with fixed pK_{a1} = 7.0 and a variable pK_{a2}, where v represents the initial rate. The pK_{a2} was obtained to be 7.21 ± 0.08. The result suggests that the protonation step with pK_a = 7.2 may be involved in the catalytic cycle. The step is likely to be the final step of the catalytic cycle shown in Scheme 1, because the step requires protonation. However, a definite assignment requires further investigation.

Experimental Procedure

General. All chemicals used in this study were commercial products of the highest available purity and were further purified by the standard methods, if necessary. $[Fe^{III}(dpaq)(CH_3CN)](ClO_4)_2$,[1] $[Fe^{II}(N4Py)(CH_3CN)](ClO_4)_2$[2] and $[Fe^{II}(tpa)(CH_3CN)_2](OTf)_2$[3] were synthesized according to literature procedures and all data were in agreement with published ones. Orange II, guaiacol, and ABTS were purchased from Aldrich. FT-IR spectra were recorded on a Shimadzu FTIR-8400 spectrometer, and UV-visible spectra were taken on an Agilent 8543 UV-visible spectroscopy system equipped with a Unisoku thermostated cell holder designed for low temperature measurements (USP-203) or with a water-jacketed cell holder thermostated by a Neslab RTE-111 water bath. ^{1}H-NMR spectra were recorded on a JEOL JMN-ECA 500 spectrometer. CSI-MS (cold-spray ionization mass spectra) and ESI-MS (electrospray ionization mass spectra) measurements were performed on a JEOL JMS-T100CS spectrometer. Elemental analyses were recorded with a Perkin-Elmer Elemental Analyzer 2400 II.

Synthesis of the H-mpaq Ligand

Synthesis of N-(2-pyridylmethyl)formamide

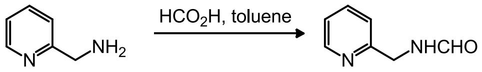

To a toluene solution (50 mL) of 2-picolylamine (4.00 g, 37.1 mmol), formic acid (3.40 g, 73.9 mmol) was added. The mixture was stirred and refluxed at 110 °C for 6 h. After the reaction was complete, saturated $NaHCO_3$ aq. and CH_2Cl_2 were added to the reaction mixture. The organic solvent was then washed with H_2O, and dried over anhydrous Na_2SO_4. After filtration, the solvent was removed. The product was obtained as a yellow oil; 3.97 g (79%). ^{1}H NMR (500 MHz, $CDCl_3$, δ): 4.58 (d, *J* = 5.7 Hz, -NHC*H*$_2$, 2H), 7.20 (dd, *J* = 7.5, 5.2 Hz, Py$_5$, 1H), 7.28 (d, *J* = 7.5 Hz, Py$_3$, 1H), 7.52 (brs, -N*H*, 1H), 7.67 (dd, *J* = 7.5, 7.5 Hz, Py$_4$, 1H), 8.30 (s, -C*H*O, 1H), 8.51 (d, *J* = 5.2 Hz, Py$_6$, 1H). ^{13}C NMR (125.8 MHz, $CDCl_3$, δ): 43.0 (-*C*H$_2$NH), 121.7 (Py$_5$), 122.2 (Py$_3$), 136.7 (Py$_4$), 148.7 (Py$_6$), 156.3 (Py$_2$), 161.4 (-*C*HO).

Synthesis of N-methyl-*N*-(2-pyridylmethyl)amine

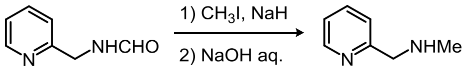

To a dry THF solution (100 mL) of *N*-(2-pyridylmethyl)formamide (3.01 g, 22.0 mmol), NaH (1.60 g, 66.1 mmol) was added in portions under nitrogen. After stirring the mixture for 15 min, CH_3I (4.69 g, 33.1 mmol) was added dropwise. After the reaction was complete (90 min), CH_3OH (20 mL) and distilled H_2O (100 mL) were added to the reaction mixture at 0 °C, and then NaOH (3.00 g, 75 mmol) was added. After the reaction mixture was refluxed overnight, the organic solvent was removed and then extracted with CH_2Cl_2. The collected organic layers were dried over anhydrous Na_2SO_4. After filtration, the solvent was removed and the residue was dried *in vacuo*. The product was obtained as a brown oil; 1.62 g (60%). ^{1}H NMR (500 MHz, $CDCl_3$, δ): 1.97 (brs, N*H*, 1H), 2.48 (s, -C*H*$_3$, 3H), 3.87 (s, -C*H*$_2$-, 2H), 7.16 (dd, *J* = 7.2, 4.6 Hz, Py$_5$,1H), 7.30 (d, *J* = 7.5 Hz, Py$_3$, 1H), 7.64 (dd, *J*= 7.5, 7.2 Hz, Py$_4$, 1H), 8.56 (d, *J* = 4.6 Hz, Py$_6$, 1H). ^{13}C NMR (125.8 MHz, $CDCl_3$, δ): 36.0 (-*C*H$_3$), 57.1 (-*C*H$_2$NH), 121.9 (Py$_5$), 122.2 (Py$_3$), 136.7 (Py$_4$), 149.2 (Py$_6$), 159.6 (Py$_2$).

Synthesis of 2-[*N*-methyl-*N*-pyridin-2-ylmethyl)]-amino-*N′*-quinolin-8-yl-acetamidate (H-mpaq)

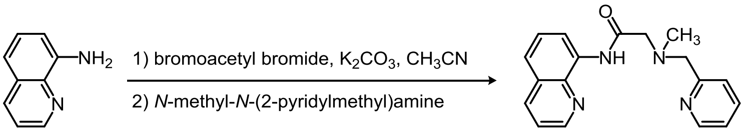

To a CH_3CN solution (50 mL) of 8-aminoquinoline (2.50 g, 17.4 mmol) and Na_2CO_3 (2.21 g, 20.8 mmol), bromoacetyl bromide (4.16 g 20.8 mmol) was slowly added under N_2, and the resulting mixture was stirred for 4.5 h at 0 °C. After removal of Na_2CO_3 through a Celite 545 pad, the filtrate was evaporated *in vacuo* to obtain a pale pink powder. The resulting powder was dissolved in CH_3CN (50 mL), to which Na_2CO_3 (1.20 g, 11.4 mol) and *N*-methyl-*N*-(2-pyridylmethyl)amine (1.1 g, 9.01 mmol) were added under N_2. The mixture was stirred overnight at 0 °C. After removal of Na_2CO_3 by a Celite 545 pad, the filtrate was evaporated *in vacuo* to obtain a viscous yellow oil. The crude product was purified by a column chromatography (Al_2O_3, hexane/ethyl acetate (1/1) to ethyl acetate as eluent). The product was obtained as a yellowish white solid; 1.20 g (41%). ^{1}H NMR (500 MHz, $CDCl_3$, δ): 2.30 (s, -C*H*$_3$, 3H), 3.42 (s, -NHC*H*$_2$CO, 2H), 3.94 (s, PyC*H*$_2$, 2H), 7.19 (dd, *J* = 7.5, 4.6 Hz, Py$_5$, 1H), 7.48 (dd, *J* = 8.0, 4.0 Hz, Qu$_3$, 1H), 7.51-7.57 (m, Qu$_5$ or Qu$_6$, 2H), 7.73 (dd, *J* = 8.0, 7.5 Hz, Py$_4$, 1H), 8.06 (d, *J* = 8.0 Hz, Py$_2$, 1H), 8.17 (dd, *J* = 8.0, 1.2 Hz, Qu$_4$, 1H), 8.54 (d, *J* = 4.6 Hz, Py$_6$, 1H), 8.81 (1H, dd, *J* = 7.5 Hz, Qu$_7$, 1H), 8.90 (dd, *J* = 4.6, 1.7 Hz, Qu$_2$, 1H), 11.51 (s, -N*H*CO, 1H). ^{13}C NMR (125.8 MHz, $CDCl_3$δ): 43.5 (-*C*H$_3$), 62.6 (-*C*H$_2$CO-), 64.2 (-*C*H$_2$Py), 116.5 (Qu$_6$), 121.6 (Qu$_3$), 121.7 (Qu$_5$ or Qu$_7$), 122.3 (Py$_5$), 123.1 (Py$_3$), 127.3 (Qu$_5$ or Qu$_7$), 128.1 (Qu$_{10}$), 134.4 (Qu$_8$), 136.2 (Qu$_4$), 136.7 (Py$_4$), 138.9 (Qu$_9$), 148.3 (Qu$_2$), 149.0 (Py$_6$), 158.7 (Py$_2$), 169.5 (*C*=O). FT-IR (ATR): 3310 (N–H), 1667 cm^{-1} (C=O). Anal. Calcd for $C_{18}H_{18}N_4O$: C, 70.57; H, 5.92; N, 18.29. Found: C, 70.53; H, 5.88; N, 18.11.

Synthesis of Iron Complexes

Caution: *Perchlorate salts of metal complexes are potentially explosive and should be handled in small quantities with care.*

Synthesis of [Fe^{III}(mpaq)(H$_2$O)$_2$](ClO$_4$)$_2$

To a solution of $Fe^{III}(ClO_4)_3 \cdot 6H_2O$ (363 mg, 0.78 mmol) in CH_3OH (2 mL) in a glass vial, a solution of H-mpaq (200 mg, 0.65 mmol) in CH_3OH (2 mL) and distilled water (60 μL) was slowly added. The dark green mixture was stirred for 2.5 hours. The precipitated green crystals were collected by filtration, washed with CH_3OH, and dried *in vacuo*. The products was isolated as a dark green powder; 195 mg (50%). ESI–MS, positive mode: *m*/*z* 392.02 $[Fe^{III}(mpaq)OCH_3]^+$. FT–IR (ATR): 1599 (C=O), 1078 and 621 cm^{-1} (ClO_4^-). UV–vis (CH_3CN): 852 nm (644 $M^{-1}cm^{-1}$), 641 nm (829 $M^{-1}cm^{-1}$), 368 nm (3420 $M^{-1}cm^{-1}$). Anal. Calcd for $[Fe(mpaq)(H_2O)_2](ClO_4)_2$ ($C_{18}H_{21}Cl_2FeN_4O_{11}$): C, 36.27; H, 3.55; N, 9.40. Found: C, 36.31; H, 3.47; N, 9.20.

Synthesis of $[Fe^{III}(mpaq)Cl_2]$

To a solution of H-mpaq (200 mg, 0.65 mmol) in CH_3OH (2 mL) in a glass vial, Et_3N (91 μL, 0.65 mmol) and a solution of $FeCl_3$ (130 mg, 0.78 mmol) in CH_3OH (2 mL) were slowly added. The dark green mixture was stirred for 3 hours. The precipitated green crystals were collected by filtration, washed with CH_3OH, and dried *in vacuo*. The products was isolated as a dark green powder; 240 mg (81%).

ESI–MS, positive mode: *m*/*z* 392.01 $[Fe^{III}(mpaq)(OCH_3)]^+$, 395.96 $[Fe^{III}(mpaq)Cl]^+$. FT–IR (ATR): 1624.1 (C=O). UV–vis (CH_3CN): 615 nm (1093 $M^{-1}cm^{-1}$), 360 nm (6813 $M^{-1}cm^{-1}$). Anal. Calcd for $[Fe(mpaq)Cl_2]\cdot H_2O$ ($C_{18}H_{19}Cl_2FeN_4O_2$): C, 48.03; H, 4.25; N, 12.45. Found: C, 48.03; H, 4.02; N, 12.09.

X-ray Crystallography. Green crystals of $Fe^{III}(mpaq)Cl_2$ were obtained by vapor diffusion of diethyl ether into the CH_3OH solution of the complex. X-ray quality single crystals were mounted on tips made from polymer films (MicroMount). The intensities were recorded on a Rigaku R-AXIS RAPID IP X-ray diffractometer using graphite-monochromatized Cu-Kα radiation (λ = 1.54187 Å), operating at 133 K. The structures have been solved by direct methods using SIR2004[4] and were refined using the Shelx-97 program package[5]. The hydrogen atoms residing in the carbon atoms were located geometrically. All non-hydrogen atoms were refined anisotropically. Important crystallographic parameters and selected bond distances/angles are listed in Tables S2 and S3.

Measurement of the peroxidase activities of iron complexes.

Oxidation of Orange II

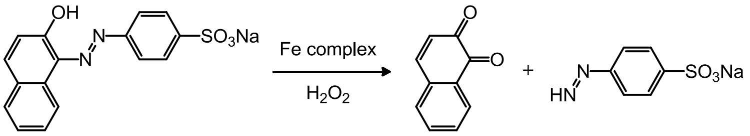

Stock solutions of Orange II, **1**–**4** or $(NH_4)_2Fe(SO_4)_2$, and H_2O_2 were prepared in 20 mM MES buffers (pH 7.0). Stock concentrations of H_2O_2 were checked before use by using $KMnO_4$. The reaction was initiated by adding H_2O_2 to the solution containing Orange II and iron complexes in a magnetically stirred, thermostatically controlled quartz cuvette at 25 °C. The initial concentrations of Orange II, iron complexes, and H_2O_2 were 20 μM, 2 μM, and 1 mM, respectively. The decrease in absorption due to the decomposition of Orange II was monitored by a UV–vis spectrophotometer at 485 nm. The initial rates were calculated using ε_{485} = 18,100 M^{-1} cm^{-1}.[6] The same reactions were also carried in the pH range of 4 to 9 in the cases of **1** and **2**. Acetate buffer, MES buffer, and TAPS buffer were used for pH-dependent experiments at pH 6.0–7.2, 7.5–8.0, and 9.0, respectively. All the measurements were triplicated.

Oxidation of Guaiacol

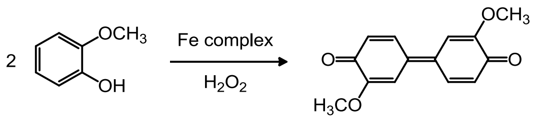

The oxidation of guaiacol was carried out at pH 7.0 by the similar procedure to the Orange II oxidation. The initial concentrations of guaiacol, iron complexes, and H_2O_2 were 2 mM, 2 μM, and 1 mM, respectively. The increase in absorption due to the tetraguaiacol formation was monitored by a UV–vis spectrophotometer at 470 nm (2.6 × 10^4 $M^{-1}cm^{-1}$).[7] All the measurements were triplicated.

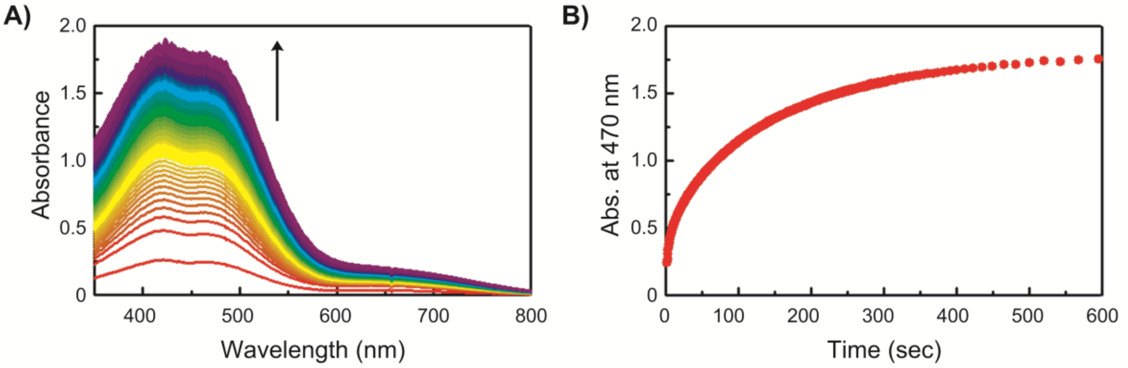

Fig S6. (A) UV–vis spectral changes for the oxidation reaction of ABTS (0.1 mM) catalyzed by 2 μM complex **1** using H_2O_2 (1 mM) in 20 mM MES buffers (pH 7.0) at 25 °C. Panel B shows the time course of the absorption at 420 nm.

Oxidation of ABTS

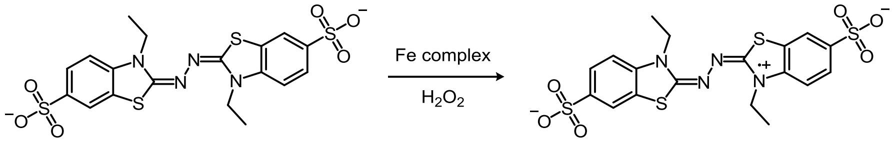

The oxidation of ABTS was carried out at pH 7.0 by the similar procedure to the Orange II oxidation. A 350 nm cut filter was used in order to avoid photooxidation of ABTS. The initial concentrations of ABTS, iron complexes,and H_2O_2 were 0.1 mM, 2 μM, and 1 mM, respectively. The increase in absorption due to the ABTS radical cation formation was monitored by a UV–vis spectrophotometer at 420 nm (3.6×10^4 M^{-1} cm^{-1}). All the measurements were triplicated.

In the case of **1**, concentrations of ABTS and H_2O_2 were varied at 12.5, 25, 50, 100, and 200 μM and at 1, 2, 4, and 8 mM, respectively. Calculation of the rate constants k_1 and $k_2k_3/(k_2 + k_3)$ were performed by a nonlinear 3D curve fitting using an Origin program package (version 8.1).

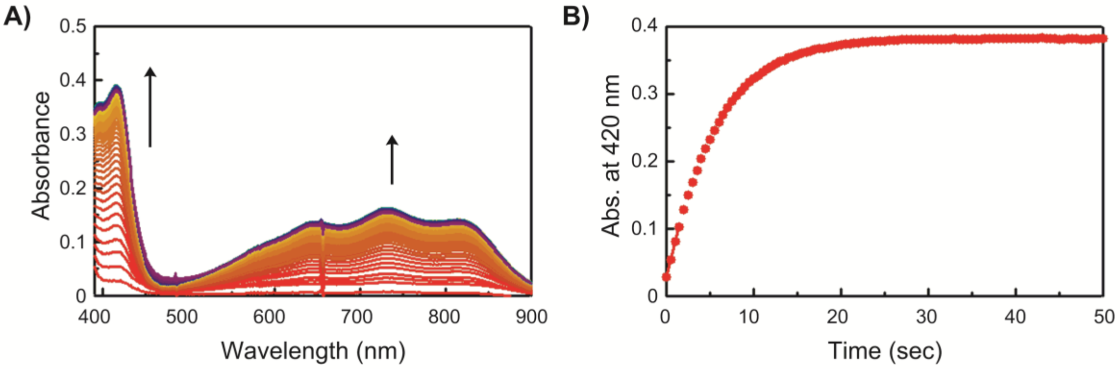

Fig S7. (A) UV–vis spectral changes for the oxidation reaction of ABTS (0.1 mM) catalyzed by 2 μM complex **1** using H_2O_2 (1 mM) in 20 mM MES buffers (pH 7.0) at 25 °C. Panel B shows the time course of the absorption at 420 nm.

CSI-MS measurement of the reaction intermediates:

Complex **1** (0.5 mM) was reacted with 100 equiv. of H_2O_2 or $H_2{}^{18}O_2$ in MeCN/H_2O (9:1) at 0 ºC. After stirring for 1 min, the reaction mixture was directly introduced to the CSI-MS probe via a Teflon capillary under N_2 pressure. Charged droplets of the sample solution were emitted from stainless steel capillary with nebulizer flow of 3.0 L/min. Instrument parameters were as follows: needle voltage 2.00 kV, orifice 1 voltage 10.0 V, orifice 2 voltage 10.0 V, ring lens voltage 10.0 V, desolvation (nebulizing) gas temperature –10 ºC.

Oxidation of Amplex Red

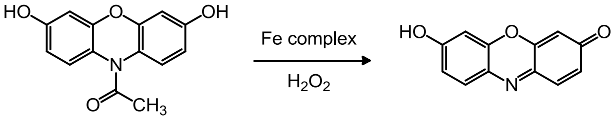

The oxidations of Amplex Red were carried out in 20 mM MES buffers (pH 7.0 and 0.5% DMSO). Amplex Red reagent and iron complexes were added to each microplate well of a 96-well plate (Thermo Scientific, 96F non-treated black mirowell). The reactions were initiated by adding H_2O_2 to the solutions. The initial concentrations of Amplex Red and H_2O_2 were 50 µM and 2 mM, respectively. Concentrations of the iron complexes were varied from 0 to 0.5 µM. The plate was gently vortexed for 100 sec at 25 °C and then the fluorescent intensity was quantified using a FilerMax F5 (Molecular Devices) with an excitation filter of 550 nm (BW 20 nm) and an emission filter of 595 nm (BW 35 nm).

Table S1. Initial Rates for Iron Complex-catalyzed Oxidation of Orange II, Guaiacol, and ABTS Using H_2O_2.

catalyst	initial rate (M s^{-1})		
	Orange II	guaiacol	ABTS
Fe(III)mpaq	$(4.03 \pm 0.05) \times 10^{-7}$	$(2.55 \pm 0.22) \times 10^{-7}$	$(1.37 \pm 0.03) \times 10^{-6}$
Fe(III)dpaq	$(2.71 \pm 0.84) \times 10^{-10}$	$(1.30 \pm 0.02) \times 10^{-10}$	$(6.27 \pm 0.29) \times 10^{-9}$
Fe(II)tpa	$(3.70 \pm 0.77) \times 10^{-10}$	$(1.05 \pm 0.05) \times 10^{-9}$	$(2.69 \pm 0.07) \times 10^{-9}$
Fe(II)N4Py	$(8.38 \pm 0.50) \times 10^{-9}$	$(1.02 \pm 0.05) \times 10^{-8}$	$(1.74 \pm 0.07) \times 10^{-8}$

Deduction of initial rate equation (1):

$$\mathrm{Fe(III)mpaq} + \mathrm{H_2O_2} \xrightarrow{k_1} \mathrm{Fe(V)mpaq}$$

$$\mathrm{Fe(V)mpaq} + \mathrm{ABTS} \xrightarrow{k_2} \mathrm{Fe(IV)mpaq} + \mathrm{ABTS}^{\cdot+}$$

$$\mathrm{Fe(IV)mpaq} + \mathrm{ABTS} \xrightarrow{k_3} \mathrm{Fe(III)mpaq} + \mathrm{ABTS}^{\cdot+}$$

Rate equation:

$$\frac{\mathrm{d[Fe(V)mpaq]}}{\mathrm{dt}} = k_1[\mathrm{Fe(III)mapq}][\mathrm{H_2O_2}] - k_2[\mathrm{Fe(V)mapq}][\mathrm{ABTS}]$$

$$\frac{\mathrm{d[Fe(IV)mpaq]}}{\mathrm{dt}} = k_2[\mathrm{Fe(V)mapq}][\mathrm{ABTS}] - k_3[\mathrm{Fe(IV)mapq}][\mathrm{ABTS}]$$

$$\frac{\mathrm{d[ABTS^{\cdot+}]}}{\mathrm{dt}} = k_2[\mathrm{Fe(V)mapq}][\mathrm{ABTS}] + k_3[\mathrm{Fe(IV)mapq}][\mathrm{ABTS}]$$

Steady state approximation is applied to Fe(IV)mpaq and Fe(V)mpaq.

$$\frac{\mathrm{d[Fe(V)mpaq]}}{\mathrm{dt}} = k_1[\mathrm{Fe(III)mapq}][\mathrm{H_2O_2}] - k_2[\mathrm{Fe(V)mapq}][\mathrm{ABTS}] = 0$$

$$\frac{\mathrm{d[Fe(IV)mpaq]}}{\mathrm{dt}} = k_2[\mathrm{Fe(V)mapq}][\mathrm{ABTS}] - k_3[\mathrm{Fe(IV)mapq}][\mathrm{ABTS}] = 0$$

Since $[\mathbf{1}]_0 = [\mathrm{Fe(III)mapq}] + [\mathrm{Fe(IV)mapq}] + [\mathrm{Fe(V)mapq}]$,

$$[\mathbf{1}]_0 = \frac{k_2[\mathrm{ABTS}]}{k_1[\mathrm{H_2O_2}]}[\mathrm{Fe(V)mapq}] + \frac{k_2}{k_3}[\mathrm{Fe(V)mapq}] + [\mathrm{Fe(V)mapq}]$$

$$= \frac{k_2k_3[\mathrm{ABTS}] + k_1(k_2+k_3)[\mathrm{H_2O_2}]}{k_1k_3[\mathrm{H_2O_2}]} \times [\mathrm{Fe(V)mapq}]$$

Thus,

$$\frac{\mathrm{d[ABTS^{\cdot+}]}}{\mathrm{dt}} = k_2[\mathrm{Fe(V)mapq}][\mathrm{ABTS}] + k_3[\mathrm{Fe(IV)mapq}][\mathrm{ABTS}]$$

$$= 2k_2[\mathrm{Fe(V)mapq}][\mathrm{ABTS}]$$

$$= 2k_2\frac{k_1k_3[\mathrm{H_2O_2}][\mathbf{1}]_0}{k_2k_3[\mathrm{ABTS}] + k_1(k_2+k_3)[\mathrm{H_2O_2}]}[\mathrm{ABTS}]$$

$$= \frac{2k_1k_2k_3[\mathrm{H_2O_2}][\mathrm{ABTS}][\mathbf{1}]_0}{k_2k_3[\mathrm{ABTS}] + k_1(k_2+k_3)[\mathrm{H_2O_2}]}$$

Table S2. Summary of Crystal Data and Intensity Collection and Structural Refinement Parameters for $Fe^{III}(mpaq)Cl_2$

	$Fe^{III}(mpaq)Cl_2$
Empirical formula	$C_{18} H_{17} Cl_2 Fe N_4 O$
Formula weight	432.11
Crystal color and habit	green block
Crystal size (nm)	0.50 × 0.10 × 0.10
Temperature (K)	133
Crystal system	triclinic
Space group	P-1
a (Å)	8.2726(10)
b (Å)	8.5344(11)
c (Å)	14.4033(18)
α (°)	72.140(2)
β (°)	84.768(3)
γ (°)	72.251(2)
Volume ($Å^3$)	921.8(2)
Z	2
D_{calc} (Mg/m^3)	1.557
Absorption coefficient, μ (mm^{-1})	1.123
Reflections collected	9489
Independent reflections [R_{int}]	4187 [0.0467]
Max. and min. transmission	0.8960 and 0.6037
Goodness-of-fit on F^2	1.044
Final R indices [$I>2\sigma(I)$]	$R_1 = 0.0497$, $wR_2 = 0.0874$
R indices (all data)	$R_1 = 0.0850$, $wR_2 = 0.0982$

Table S3. Selected Bond Lengths (Å) and Angles (deg) for $Fe^{III}(mpaq)Cl_2$.

	$Fe^{III}(mpaq)Cl_2$
Fe(1)-N(3)	2.051(2)
Fe(1)-N(1)	2.111(2)
Fe(1)-N(2)	2.174(2)
Fe(1)-N(4)	2.196(2)
Fe(1)-Cl(2)	2.3073(9)
Fe(1)-Cl(1)	2.3138(10)
C(15)-O(1)	1.221(4)
N(3)-Fe(1)-N(1)	77.20(10)
N(3)-Fe(1)-N(2)	92.51(10)
N(1)-Fe(1)-N(2)	90.29(9)
N(3)-Fe(1)-N(4)	75.30(9)
N(1)-Fe(1)-N(4)	149.10(10)
N(2)-Fe(1)-N(4)	77.17(9)
N(3)-Fe(1)-Cl(2)	174.54(8)
N(1)-Fe(1)-Cl(2)	100.16(7)
N(2)-Fe(1)-Cl(2)	82.68(7)
N(4)-Fe(1)-Cl(2)	105.97(7)
N(3)-Fe(1)-Cl(1)	92.85(8)
N(1)-Fe(1)-Cl(1)	99.47(7)
N(2)-Fe(1)-Cl(1)	169.70(7)
N(4)-Fe(1)-Cl(1)	95.73(7)
Cl(2)-Fe(1)-Cl(1)	92.30(4)
N(3)-Fe(1)-N(1)	77.20(10)

References

1. Y. Hitomi, K. Arakawa, T. Funabiki and M. Kodera, *Angew. Chem. Int. Ed.* 2012, **51**, 3448.
2. M. Lubben, A. Meetsma, E. C. Wilkinson, B. Feringa and L. Que, Jr. *Angew. Chem., Int. Ed. Engl.* 1995, **34**, 1512−1514.
3. A. Diebold and K. S. Hagen, *Inorg. Chem.* 1998, **37**, 215.
4. M. C. Burla, R. Caliandro, M. Camalli, B. Carrozzini, G. L. Cascarano, L. De Caro, C. Giacovazzo, G. Polidori and R. Spagna, *J. Appl. Cryst.* 2005, **38**, 381-388.
5. G. M. Sheldrick, Univ. of Göttingen: Göttingen, 1997.
6. W. C. Ellis, C. T. Tran, M. A. Denardo, A. Fischer, A. D. Ryabov and T. J. Collins, *J. Am. Chem. Soc.* 2009, **131**, 18052.
7. S.-i. Ozaki and P. R. Ortiz de Montellano, *J. Am. Chem. Soc.* 1995, **117**, 7056.